Persistence at Full Ocean Depth

Mathieu Kemp, Matt Palanza, Cheryl Skibski, Josh Ormsby, and Michelle Estaphan
Bluefin Robotics LLC
Corresponding author: mkemp@bluefinrobotics.com

Abstract—This paper introduces a station-keeping technique called Sprint-and-Drift, applicable for extended-duration barrier detection missions at extreme depths. The technique allows a UUV to station-keep at very low power, without being tied to the seafloor. Two of the enabling technologies, the high resolution variable buoyancy system, and the algorithm that controls the VBS, are described in detail.

Keywords: UUV, persistence, station-keeping, buoyancy control, anti-submarine warfare.

I. INTRODUCTION

A large fraction of the UUV research and development investments to this day have been allocated to mine-counter-measure missions (MCM). The recent award of an MCM-UUV acquisition contract by the US Navy [1] signals the end of a phase, and an imminent shift away from MCM and towards anti-submarine warfare (ASW) and Intelligence Surveillance Reconnaissance (ISR) applications [2,3,4].

The shift from MCM to ASW/ISR comes with order of magnitude increases in the spatio-temporal scales, from 10-30 hours/10-50km for MCM to 30-120 days/500-2000km for ASW/ISR. Current UUV capabilities are well below these levels.

There are two gaps between needs and capabilities. The first is energy: Extending mission duration will require substantial advances in the areas of energy density, vehicle drag, propulsive efficiency, energy management, and hotel/payload power.

The second technology gap is reliability. Reliability metrics such as mean-time-between-failure, which are ubiquitous in the automotive or consumer electronics industries, have historically not been a primary concern of UUV designers. One exception is the work by the Southampton group [5]. One might argue that past focus on MCM is responsible for this general lack of attention. Regardless, major advances in the areas of autonomous fault detection, fault classification, and fault recovery will be needed before UUVs can support ASW/ISR missions [6]

The seminal work by MBARI on the Tethys platform [7] showed that substantial improvements are achievable with proper attention paid to drag, propulsive efficiency, and energy management alone. Their work was specifically targeted at ocean sensing missions, i.e. 5-10W payload ranges. For ASW or ISR, where payloads are the range 50-500W, the gap cannot be filled with platform enhancements alone. Energy storage technology will require a quantum jump; in connection with this, the Office of Naval Research recently initiated a long-term program that will ultimately produce UUV batteries in the 800-1800 kWh range [3].

In this paper we discuss an energy-management technique, called Sprint-and-Drift, specifically developed for a UUV-based ASW barrier detection system at full ocean depth. The technique reduces vehicle power from 250W to 10W, enabling multi-month ASW deployments. We emphasize that the technique only works in low-current environments, such as those often encountered at abyssal depths, and that it does not rely on the development of next-generation energy technology.

The paper is organized as follows: Section 2 discusses the energy management technique. Section 3 discusses its algorithmic implementation, and Section 4 discusses its hardware implementation.

II. SPRINT-AND-DRIFT

A. Context

The context for the energy management technique presented here is ASW barrier detection. In UUV-based barrier detection, multiple UUVs combine to form a protective grid. Given the scale of ASW, the grid would normally require a large number of vehicles. One way to get around this is to operate below the critical acoustic depth – near 4500m – in order to take advantage of the large detection radii enabled by ray bending [8]. To maximize detection performance, the UUVs would be required to maintain at least a 50m gap with the seafloor, and to periodically ascend to the critical depth.

As discussed in the introduction, ASW has very long durations and large payloads, both of which require the vehicle to run on very low power levels. In deep-barrier detection, the vehicle is also required to transit to its assigned location, then to station-keep for a long duration, and to ascent periodically to the critical depth.

Consider a winch-based solution: the vehicle would transit to its assigned location, then drops an anchor to save on power, and periodically winch itself up and down to the critical depth. This solution uses no power to station-keep, and it is ideal from a navigation standpoint since the vehicle cannot get "lost". On the other hand, catenary calculations performed using a typical current profile indicate the need for a 3-4,000m tether for the 1,500m ascent to the critical depth. The tether/winch system would therefore have to be large, it would be prone to entanglement, and it would also restrict the UUV's horizontal mobility. Since the UUV would need to carry an anchor, it would be either negatively buoyant during transit, or it would have to jettison a large amount of flotation. Despite the power savings, this solution is not practical.

B. *Sprint-and-Drift*

Consider now the solution in Figure 1: the vehicle transits to its assigned location, drops a beacon, and starts a "Sprint-and-Drift" cycle: during the drift phase, it kills all power and drifts with the current, and during the sprint phase it swims back to the beacon. Sprint-and-Drift is entanglement-free, and it doesn't require an anchor or jettisoning flotation.

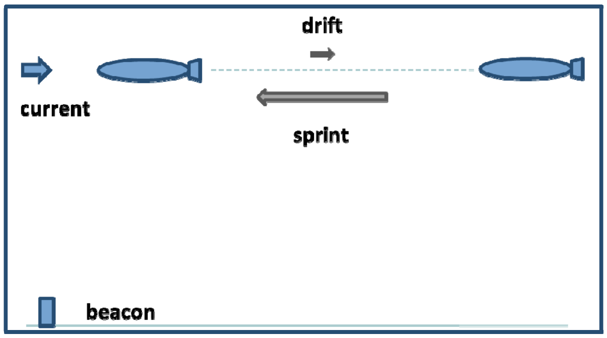

Figure 1. Sprint-and-Drift. During the drift phase, power to the vehicle is off, and the vehicle drifts with the current. After a set time, the vehicle wakes up and sprints back to the beacon.

Sprint-and-Drift is not a zero-energy solution unlike the winch-based approach. The question is, how much energy does it require?

Sprint-and-Drift capitalizes on two observations:

- Shutting down the propeller periodically and sprinting back saves more energy than swimming against the current at constant speed. There is in fact a "sweet spot" where power consumption is very small (Figure 2).
- The scale of ASW is such that a 1km navigation uncertainty is acceptable. The vehicle does not need to know where it is precisely. As a result, navigation sensors are not needed at all during the drift phase, provided the drift distance does not exceed the range of the beacon and that the vehicle stays clear of the seafloor.

Let us elaborate on the first observation. We consider a setup where the drift distance is *D*, the current is *C*, power during the drift phase is P_{drift} , and power during the sprint phase is P_{sprint}. The time-averaged power over a Sprint-and-Drift cycle is:

$$\langle P \rangle = \frac{P_{\text{sprint}} T_{\text{sprint}} + P_{\text{drift}} T_{\text{drift}}}{T_{\text{sprint}} + T_{\text{drift}}} \qquad (1)$$

Average power is a function of speed-over-ground: During the sprint phase, power is the sum of the sprint hotel load and of propulsive power, $P_{\text{sprint}} = H_{\text{sprint}} + K\left(U + C\right)^3$, where *U* is speed-over-ground, and *K* is proportional to the drag area and inversely proportional to propulsive efficiency. The duration of the sprint phase is a function of the vehicle's speed, $T_{sprint} = D/U$.

During the drift phase, the propulsive power is zero. The only power used is the drift hotel load, $P_{\text{drift}} = H_{\text{drift}}$. The duration of the drift phase is a function of the current, $T_{drift} = D/C$.

Figure 2 shows the dependence of the average power <*P*> on speed-over-ground for typical deep ocean conditions. At the sweet spot (0.6m/s), the minimum power is 7W. By comparison, a vehicle swimming at 1.5 m/s would consume 250W.

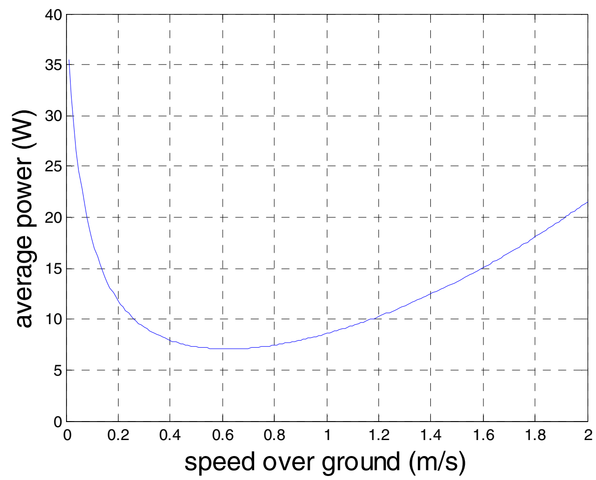

Figure 2. Dependence of average power on vehicle speed over ground. The minimum power, 7W, is reached at 0.6 m/s. Conditions: 0.15 kts current, 21" diameter, 0.3 drag coefficient , 40W hotel during sprint, 0.5W hotel during drift, 60% propulsive efficiency.

This 30-fold reduction has two causes: 1. reducing the speed reduces the propulsive power, and 2. the low-duty cycle allowed by Sprint-And-Drift reduces the mean hotel load by 90%.

Further examining Equation 1, if the electronics were completely off during the drift phase, the minimum average power would be entirely determined by sprint hotel power:

$$\langle P \rangle_{\min} = \text{duty cycle} \cdot 1.5 \cdot H_{\text{sprint}} \qquad (2)$$

How small could the hotel sprint power be? Based on the second observation, the vehicle needs to:

1. measure range/bearing to the beacon and speed-over-ground/altitude at the end of the drift phase,

2. measure depth + heading + pitch during the sprint phase,

3. measure range/bearing to the beacon and speed-over-ground/altitude at the end of the sprint phase.

Range and bearing to the beacon could be measured with an inverted USBL, an LBL, or a USBL: iUSBL is advantageous because it has no surface expression, LBL requires surveying of the beacons, and USBL requires continuous surface presence. With appropriate power management, 7W time-averaged/ 40W instantaneous sprint hotel does not appear unrealistic.

III. TOLERANCE ON NEUTRALITY

A. Requirement

One of the effects of drifting with the current is that any deviation from neutral buoyancy–called *residual buoyancy* in what follows– causes vertical drift.

From a system impact, how much vertical drift is acceptable? For acoustic reasons (Section 2), the vehicle must maintain at least a 50m gap from the seafloor. The need for DVL ground lock sets the upper bound at ~150m. If we require a 10m safety margin on either side, then the vehicle can at most drop from 100m to 60m, or ascend from 100 to 140m. Thus, the maximum vertical drift is 40m.

Figure 3 provides a sense of the scale involved: to stay within the maximum 40m vertical drift after 20 minutes, the buoyancy residual must be less than 0.5lbs. Meeting this specification, will require a high resolution variable buoyancy system (VBS) – discussed in the next Section – and a buoyancy control algorithm capable of corralling the VBS's resolution – discussed next.

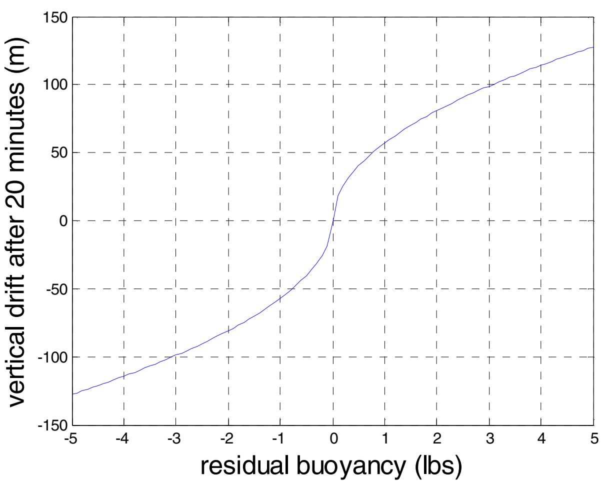

Figure 3. Dependence of vertical drift on residual buoyancy after 20 minutes. To maintain the drift below 40m, the residual must be less than 0.5 lbs. Conditions: 23'L x 21"D vehicle, 1.0 cross-drag coefficient.

B. Buoyancy algorithm

In Sprint-and-Drift, the role of the VBS is to null the buoyancy–instead of active depth control. The power required for active depth control at 6000m would be prohibitive, and would in fact be wasted, since depth can be adjusted at a lower cost during the sprint phase.

The vertical equations of motion are:

$$m\frac{dw}{dt} = B - k\left|w\right|w \qquad \frac{d\Delta B}{dt} = \phi u \tag{3}$$

The first equation is Newton's law: w is the vertical rate of ascent, m is the effective mass (dry mass + entrained water + added mass), B is the residual buoyancy. The last term is drag along the vertical axis, where k is a constant proportional to vehicle diameter and vehicle length. The second equation describes a constant flow rate VBS like the one described in the next Section. The rate of change of the residual buoyancy is equal to a flow rate ϕ, modulated by a quantity u under control of the buoyancy algorithm.

As explained in Section 4, the VBS under consideration has a constant flow rate. It can either be closed (u=0), increasing the buoyancy (u=+1), or decreasing the buoyancy (u=-1). Given these constraints, proportional control is not possible. Instead, the system requires bang-bang control:

$$u = \begin{cases} -1 & \tilde{B} > threshold \\ +1 & \tilde{B} < -threshold \\ 0 & \left|\tilde{B}\right| < threshold \end{cases} \tag{4}$$

where the buoyancy estimator $\tilde{B}$ is, based on the first equation of motion:

$$\tilde{B} = \tilde{m}\dot{w} + \tilde{k}\left|w\right|w \tag{5}$$

An approximate value of $\tilde{m}$ can be derived from a measurement of vehicle volume and from the added mass of a cylinder of similar size. An approximate value of $\tilde{k}$ can be derived from the drag coefficient of a cylinder in cross-flow. Refined values can be obtained by direct measurement of depth versus time on the actual vehicle with known residual buoyancy followed by parameter identification.

The control laws Eqs 4-5 requires measuring the ascent rate and acceleration. The only acceptable sensor is depth given the mission profile: INS and DVL are unacceptable for energy reasons, also because of loss of ground lock during the excursions to the critical depth. Low-power accelerometers are not acceptable given their sensitivity compared with the sub-milli-g vertical accelerations due to the residual buoyancy.

C. Performance of algorithm

Figure 4 shows the phase-space vector field corresponding to the equations of motion (Eq. 3) with perfect buoyancy estimation ($\tilde{B} = B$). Independent of the initial condition, the flow-lines converge to a point on the terminal velocity line, with the converged buoyancy less than or equal to the threshold.

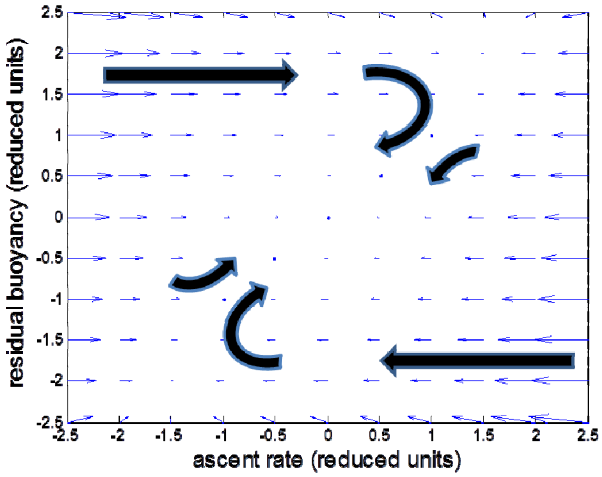

Figure 4. Flow vector field in phase space. The variables are in a system of units where m=k=ϕ=1. The flow converges to the terminal velocity line.

We analyzed the sensitivity of convergence to parameter error, and found that provided the initial ascent rate is bounded from above and that the relative error of the estimated parameters is less than:

$$\frac{\delta\left(\tilde{m}/\tilde{k}\right)}{\tilde{m}/\tilde{k}} < \frac{threshold}{kw_{\max}^2} \qquad (6)$$

then convergence is preserved. Using values representative of a 21" vehicle, the 0.5lbs threshold requirement, and assuming that the initial rate of ascent is <10cm/s, convergence is guaranteed provided $\tilde{m}/\tilde{k}$ if off by less than 10%.

Figure 5 shows the performance of the algorithm when noise due to sensor quantization is also included. Provided that the buoyancy is estimated at a low enough rate, and that the depth sensor's *quantization*period* product is high enough, performance is not affected.

Let us elaborate: The buoyancy estimator in Equation 5 depends on ascent rate and acceleration. These are measured by finite-differencing of the depth data. Sensor noise introduces error in these measurements. The error is a function of sensor noise and of the period between buoyancy estimations. If we consider high-quality deep-rated depth sensors, such as the Paroscientific 8000 series, the main source of error is sensor quantization (called *resolution* in the manufacturer's datasheet). The quantization level is user-controllable, however the product *quantization*period* is constant.

The ascent rate and ascent acceleration error due to sensor quantization and estimation period is:

$$\varepsilon\left(\text{ascent rate}\right) = O\left(\Delta z/T\right)$$
$$\varepsilon\left(\text{ascent acceleration}\right) = O\left(\Delta z/T^2\right) \qquad (7)$$

where K is a constant equal to the *quantization*period* product, and T is the buoyancy estimation period. The dependence of the error on T is strong, $1/T^2$, and is the means of controlling the error level.

We now ask, What sets the minimum buoyancy estimation sampling period? The buoyancy requirement of 0.5lbs can only be met provided the buoyancy estimator it as least as accurate. This condition leads to: $T > \sqrt{\Delta B/m\Delta z}$. Sensor resolution is determined by the vehicle's pitch and heading dynamic control loop rate. Using 10Hz gives 1mm for a 7000m sensor. Assuming a 2000kg vehicle, this gives T>1s.

We also ask, How does noise affect convergence? Sensor noise affects the buoyancy estimator. Given the bang-bang nature of the algorithm, the error has no impact except in the phase-space region near the threshold line. and convergence is not affected (Figure 5). The only impact of noise is its effect on the actual converged value, and as we showed in the previous paragraph the fluctuations can be made arbitrarily small by increasing the estimation period.

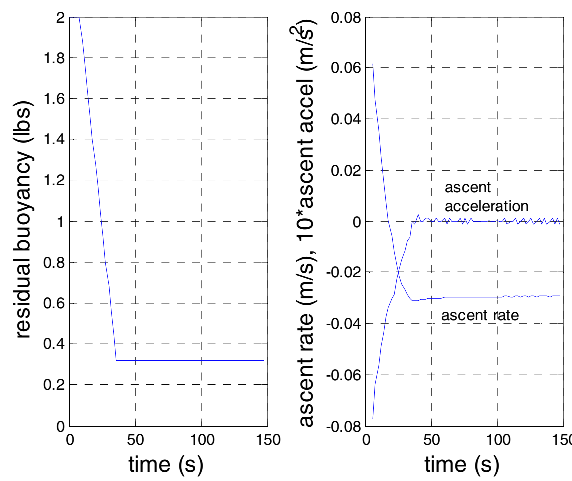

Figure 5. Performance of the buoyancy control algorithm. Left: the residual buoyancy drops from its initial value of 2lbs, to within the threshold of 0.5lbs. Right: the noise in the ascent rate and ascent acceleration due to sensor quantization does not affect performance. The data was generated using a 6DOF vehicle model, with 10% error in the buoyancy estimation parameters, with an initial ascent rate of 10cm/s, and a sensor setting of 0.5mm quantization / 10Hz sampling rate, and date under-sampling at 0.5Hz.

IV. Variable Buoyancy System

A. Design requirements

The following VBS requirements were derived after a system-level analysis of the vehicle:

- Capable of operating in the range 0 to 6000m
- 0.5lbs resolution

- 10L dynamics range
- 1 lbs/min flow rate
- 900W max power

B. Design

The VBS is a stand-alone section of the 21” ASW UUV (Figure 6). The bulk of the components are mounted inside a 6,000 m depth rated, 17” glass sphere. The pressure-balanced external oil storage system is external to the sphere. Wherever possible, all components in the VBS are COTS and rated to 10,000psi. The only exception is the anti-siphoning device, which we will discuss in detail later.

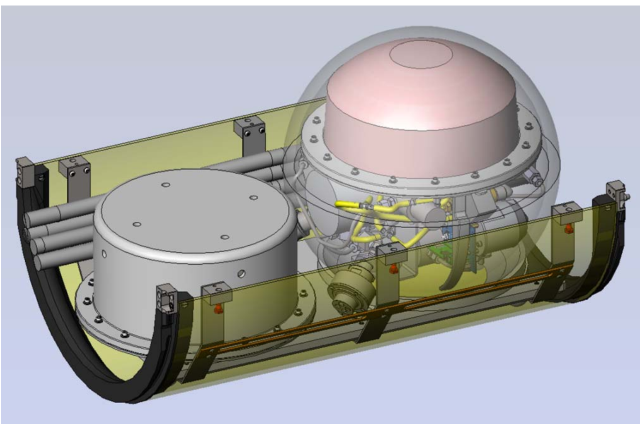

Figure 6. 21” Variable Buoyancy System vehicle section.

The VBS is a closed-loop hydraulic system, in which a constrained volume of oil is moved between an internal and an external bladder. Figure 7 shows a conceptual representation. The hydraulic pump, a Dynex PF501, was specified to be capable of a flow rate of at least 0.1 gallons per minute at 10,000psi. It has a relatively low input power requirement, which can be further reduced by disabling two of the four pistons. An electric motor is matched to the pump. In order to move oil outside the sphere, the electric motor turns the hydraulic pump, which pushes oil out through a one-way check valve, a backflow valve, and into the external bladder. Oil flow is estimated by measuring mechanical rotations of the constant displacement pump. A vacuum sensor is used to detect an empty internal bladder condition. Oil is returned by opening a sequence of two hydraulic valves: a high-pressure valve is first opened to allow a dual pressure-reduction stage to step down the pressure seen by a second low-pressure valve. The low-pressure valve is then opened and oil flow is measured directly as it enters the internal bladder. The return flow rate is dependent on external pressure, and can be adjusted with the two pressure regulators.

The “backflow valve”, mounted as a penetrator through the sphere, is a custom anti-siphoning device. It is designed to close when a small differential between the oil system and the ocean occurs. It provides a mechanical safety stop in the event that the external bladder is fully drained of oil, preventing the external bladder from extruding into the hydraulic system. The differential pressure is adjustable by changing spring constants.

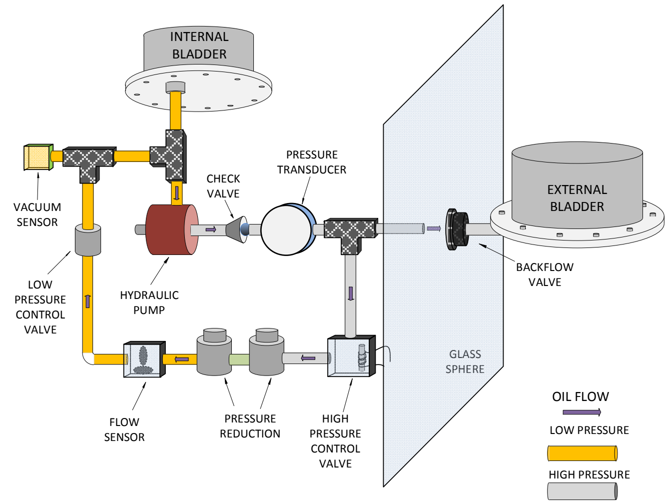

Figure 7. Variable Buoyancy System block diagram.

A tabletop version of the system was assembled for lab testing using the actual design's system components pushing against an accumulator capable of the full range of pressures (Figure 8). This test-bed was designed and built to allow a nearly complete VBS to operate in an environment that closely models the operating conditions. The test-bed consisted of: all internal electrical and mechanical components of the VBS, a system designed to emulate ocean pressure, and a control and data acquisition system. The test-bed permitted full system characterization, component testing, and integration, allowing us to de-rate the risks associated with the design. Readily available general purpose test equipment was used to measure and log test data.

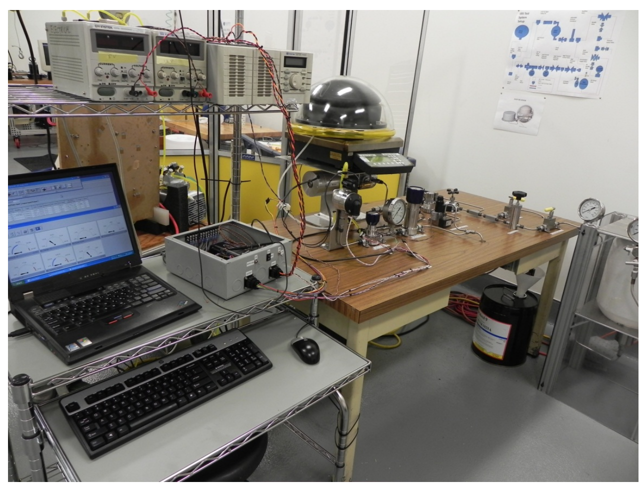

Figure 8. VBS test-bed

Two fundamental requirements needed to be verified in testing: 1) the ability to start the pump and to constantly pump against all expected environmental pressures, and 2) proper control of oil pressure and flow rate back into the system against all expected environmental pressures.

The external environment was simulated with a 2.5 gallon capacity 10,000psi hydraulic accumulator. The accumulator was used for both output flow and return flow testing. In testing the output capacity, the accumulator provided two functions: a smoothing filter effect, and a constant pressure reserve. In flow return testing, the accumulator provided an extended reserve of pressure.

C. Results

1) Flow rate and power

The data acquisition system automatically logged: time, system voltage, system current, external pressure, input pressure, motor speed, and oil flow. Output flow was measured and calibrated in two ways: First, the hydraulic output of the VBS was pumped against the external accumulator through a pressure relief valve. The output of the pressure relief valve was fed back into the system and measured directly by the flow meter. Testing exhibited the hysteresis of the pressure relief valve – care was taken to measure only the output of the pump itself and not oil flow returning from the accumulator reserve. The second method used a scale under the internal bladder. Time was measured while a measured weight displacement was pumped against accumulator pressure.

Figure 9 shows outgoing and incoming flow versus pressure. The outgoing flow varied from 0.1gpm at 5500psi to 0.6gpm at 9,000psi. The incoming flow was pressure-dependent, decreasing from 0.02gpm at 8,500psi to 0.17gpm at 5,500psi.

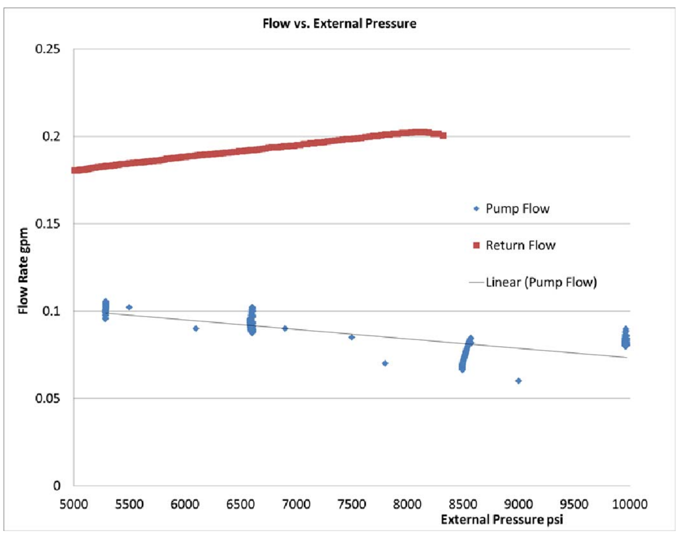

Figure 9. Output and return flow rate vs external pressure at 2200rpm.

Figure 10 shows the dependence of power and flow rate on motor speed at 10,000psi. As expected, both quantities increased linearly with motor speed. The maximum power was 700 Watts, below the requirement.

2) Issues encountered during testing

Testing exposed the following issues:

1. The initial bladder design was based on a system similar to that used in the Spray glider. It consisted of two fiber reinforced rubber layers, bonded together in a spherical shape. Early prototypes failed consistently during capacity testing, a 10psi differential on the bladder causing material separation. After multiple attempts and failures at improving this design, the approach was abandoned. We moved instead to a mechanical assembly, similar to that used in several other pressure compensation devices: an aluminum base plate with an industrial rolling diaphragm, bolted together with a ring to create clamping pressure. This design change was successful.

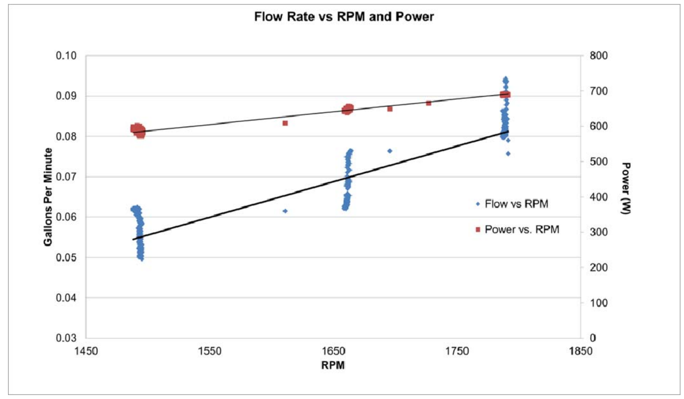

Figure 10. Results of the RPM sweep test. Due to hardware availability issues at the time of this test, maximum test speed was limited to 2000rpm.

2. The backflow valve was closing under two conditions: A shock to the hydraulic system, which appeared when the high pressure control valve was opened, causing the backflow valve to be suddenly exposed to the high differential with the internal side of the hydraulics. The shock slammed the valve shut and the pressure differential kept it closed. We solved this by adding a low-pressure control valve immediately behind the pressure reduction stages. Sequentially opening the high, then the low pressure control valves, effectively dampened the shock. We also found that in constant oil return, high flow rates would shut the backflow valve. Stepping the spring rate from a 2psi differential to 10psi was successfully tested up to 10,000psi and flow rates up to 0.2gpm.

3. Manufacturer data stated that the hydraulic pump did not require any inlet pressure. Further discussions with the manufacturer's technical staff indicated the need for at least 2-5psi. We verified this in testing, and found that pump performance greatly improves with small amounts of inlet pressure. Figure 10 shows an example: before t=2000s, the pump is running with no inlet pressure and the flow is low (green trace, 0.04gpm). At t=2000s, we temporarily manipulated the control valves to apply 12psi at the pump, and the flow jumped to 0.09gpm.

V. SUMMARY

The paper introduced a station-keeping technique called Sprint-and-Drift, which is currently being implemented for an ASW application at extreme depths. Sprint-and-Drift allows a UUV to station-keep at very low power levels, without being tied to the seafloor. The paper discussed in detail two of the enabling technologies: a high-resolution variable buoyancy system, and an algorithm to control the VBS.

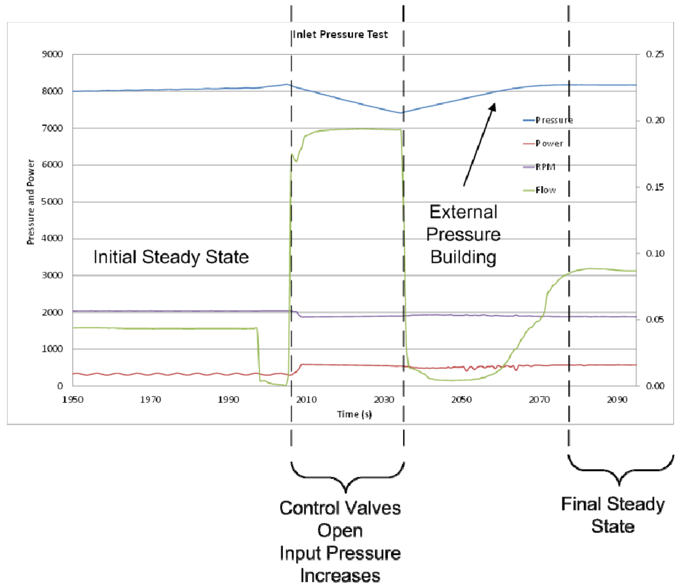

Figure 11. Input pressure test results: at t=2000s, a minor manipulation of the control valves allows the flow to increase from 0.04 to 0.09gpm.

VI. REFERENCES

[1] Official notice of SMCM-UUV contract award available onine at: http://www.defense.gov/contracts/contract.aspx?contractid=4634, and http://www.gd-ais.com/News/US-Navy-Awards-General-Dynamics-87-Million-for-Unmanned-Underwater-Mine-Countermeasure-Vehicle-.xml.

[2] J. Smith, R. Lindman, "Proteus - Large Diameter Undersea Vehicle and it sApplications for Undersea Warfare, 10th MINWARA Symposium, 2012. Available online at: http://www.10thsymposium.com/presentations/Wed%20pm%20B/1530-1600%20Smith%20Bluefin%20-%20Proteus%20-%20MINWARA%20-%20%20050912.ppt%20%5BRead-Only%5D.pdf.

[3] LDUUV program thresholds and objectives published in ONR-BAA-11-025, "Large Displacement Unmanned Underwater Vehicle Innovative Naval Prototype Technology", 2011. Available online at http://www.onr.navy.mil/~/media/Files/Funding-Announcements/BAA/2011/11-025.ashx

[4] DSOP program objectives published in DARPA-BAA-11-24. Available online at https://www.fbo.gov.

[5] G. Griffiths, N. Millard, S.D. McPhail, P. Stevenson, P. Challenor, "On the Reliability of the Autosub Autonomous Underwater Vehicle", Southampton Oceanography Centre Research and Consultancy Report,(48)), 2000Most of the UUV research and development dollars to this day have been allocated for mine-countermeasures (MCM) missions. Viewed from this perspective, the award of an MCM-UUV acquisition contract by the US Navy [1] might be a precursor to a shift in the UUV R&D landscape, away from MCM, and towards anti-submarine warfare (ASW) and Intelligence Surveillance Reconnaissance (ISR) missions [2,3,4].

[6] See for example:. J. Ernits, R. Dearden, "Fault Diagnosis Challenge in a Flight-Class Autonomous Underwater Vehicle", Proceedings of the 22nd International Workshop on the Principles of Diagnosis, 2011.

[7] J.G. Bellingham, Z. Yanwu, J.E. Kerwin, J. Erikson, B. Hobson, B. Kieft, M. Godin, R. McEwen, T. Hoover, J. Paul, A. Hamilton, J. Franklin, A. Banka, "Efficient Propulsion for the Tethys Long-Range Autonomous Underwater Vehicle", Proceedings of Autonomous Underwater Vehicles Conference, 2010.

[8] F. Jensen, W. Kuperman, M. Porter, H. Schmidt, "Computational Ocean Acoustics", Modern Acoustics and Signal Processing, AIP press, 2000.

ACKNOWLEDGMENTS

We thank Andy Coon for his continuous support of the program. This work was funded by DARPA STO.